# Cubam receptor-mediated endocytosis in hindgut-derived pseudoplacenta of a viviparous teleost *Xenotoca eiseni*

Atsuo Iida[1,*], Kaori Sano[2], Mayu Inokuchi[3], Jumpei Nomura[1], Takayuki Suzuki[1], Mao Kuriki[4], Maina Sogabe[4], Daichi Susaki[5], Kaoru Tonosaki[5], Tetsu Kinoshita[5], Eiichi Hondo[1]

1. Department of Animal Sciences, Graduate School of Bioagricultural Sciences, Nagoya University, Tokai National Higher Education and Research System, Nagoya, Aichi, Japan.
2. Department of Chemistry, Faculty of Science, Josai University, Sakado, Saitama, Japan.
3. Department of Life Sciences, Toyo University, Itakura, Gunma, Japan.
4. Department of Regeneration Science and Engineering, Institute for Frontier Life and Medical Sciences, Kyoto University, Kyoto, Kyoto, Japan.
5. Kihara Institute for Biological Research, Yokohama City University, Yokohama, Kanagawa, Japan.

**Correspondence**: Atsuo Iida

**E-mail**: tol2.4682@gmail.com

**Author contribution**: A.I. designed the study. A.I., K.S., M.I., and JN carried out the experiments. T.S., M.K., and M.S. contributed to fluorescent microscopy. D.S., K.T., T.K., and E.H. contributed to next-

generation sequencing and data analysis. A.I. wrote the manuscript.

**Competing interest statement**: The authors declare that they have no competing interests.

**Keywords**: viviparity, teleost, Goodeidae, pseudoplacenta, endocytosis, proteolysis

**This PDF file includes**:

Main Text

Figures 1 to 5

**Abstract**

Nutrient transfer from mother to the embryo is essential for reproduction in viviparous animals. Here, we focused on the molecular mechanism of nutrient absorption in hindgut-derived pseudoplacenta (trophotaenia) of the viviparous teleost *Xenotoca eiseni*. The candidate genes involved in the process were identified by RNA-Seq, and then protein distribution and functions were investigated using molecular biological methods. Our results suggested that Cubam (Cubilin-Amnionless) receptor-mediated endocytosis and cathepsin L-dependent proteolysis are involved in the maternal macromolecule absorption via the trophotaenia. Such a nutrient absorption mechanism involving endocytosis is not a specific trait to viviparous fish. Similar processes have been reported in the larval stage of oviparous fish or the suckling stage of viviparous mammals. Our findings suggest that the viviparous teleost acquired trophotaenia-based viviparity via a modification of the intestinal absorption system common in vertebrates. This is a fundamental study to understand the strategic variation in the reproductive system of vertebrates.

## Introduction

August Krogh wrote, "*For such a large number of problems there will be some animal of choice or a few such animals on which it can be most conveniently studied*" [1]. This study aimed to investigate the molecular mechanism of maternal nutrient absorption in a species-specific pseudoplacenta of a viviparous teleost species belonging to the family Goodeidae.

Viviparity is a reproduction system, whereby the oocyte is fertilized in the female body, and subsequent embryo growth occurs with maternal component supply. Each viviparous animal has acquired processes specialized to the gestation in both the mother and embryo [2]. The placenta and umbilical cords in viviparous mammals are major components of the process for mother-to-embryo material transport [3,4]. Other viviparous components such as the extended yolk sac or pseudoplacenta are known in several viviparous vertebrates, except mammals [5].

The family Goodeidae is a freshwater small teleost distributed in Mexico, which includes approximately 40 viviparous species [6]. They possess trophotaenia, which is a hindgut-derived pseudoplacenta that absorbs the maternal component [7,8]. Trophotaenia is a ribbon-like structure consisting of a single epithelial layer, internal blood vessels, and connective tissues [9,10]. The epithelial cell is like an enterocyte in the intestine. Electron microscopy indicated that microvilli form in the apical side of the cell and intracellular vesicles in the cytoplasm [11]. Since the 1980s, these structures have been believed to be involved in maternal component absorption [12]. The nature of the maternal component was predicted to be proteins or other macromolecules secreted into the serum or ovarian fluids; however, no one has experimentally determined its distinct component [13,14]. Recently, we demonstrated that a yolk protein vitellogenin is secreted into the ovarian lumen of pregnant females, and the intraovarian embryo absorbs the nutrient protein via the trophotaenia using a goodeid species *Xenotoca eiseni* [15]. In that study, enterocyte-like microvilli and intracellular vesicles were also observed in the epithelial cells of the

trophotaenia. We hypothesized that the epithelial layer cell in the trophotaenia absorbs the maternal protein and/or other components as macromolecules because the ovarian lumen lacks proteolysis activity like the digestive intestine. However, the molecules responsible for the trophotaenia-mediated macromolecule absorption have not been reported.

Vacuolated enterocytes involved in macromolecule absorption have also been reported in other vertebrate species, including suckling mammals and stomachless fish [16-18]. Park et al. [19] reported that the scavenger receptor complex Cubam (Cubilin-Amnionless) and Dab2 are required for macromolecule uptake in zebrafish juveniles. Furthermore, the conditional knockout of *Dab2* in mice led to stunted growth and severe protein malnutrition at the suckling stage [19]. Based on this report, we discuss the commonality of molecular process for the macromolecule absorption between the intestinal enterocytes and the trophotaenia [15]. However, the molecules responsible for macromolecule absorption in the trophotaenia are still elusive.

Here, we report candidate molecules for nutrient uptake and subsequent proteolysis in the trophotaenia of *X. eiseni*. An RNA-Seq for trophoteniae indicated candidate receptor molecules and endocytosis-associated proteases expressed in the trophotaenia. Immunohistochemistry and biochemical assays suggested the presence and functions of the candidate factors in the trophotaenia.

## Results

### *Gene expression in trophotaenia*

Our previous findings and the hypothesis based on that are described in Figure 1A. In a viviparous teleost, *X. eiseni*, the embryo is raised in the ovary while receiving maternal nutrients. The trophotaenia is a pseudoplacenta that plays a role in the absorption of maternal nutrients consisting of proteins and other supplements. Based on previous studies, we hypothesized that several maternal proteins are absorbed by endocytosis-mediated proteolysis in the epithelial cells of the trophotaenia. To verify this hypothesis, we explored candidate genes for receptor, adaptor, vesicle, and protease proteins that are highly expressed in the trophotaenia. RNA-Seq analyses were performed using total RNA extracted from the trophotaeniae of the 3rd- or 4th-week embryos (Figure 1B). We selected candidate genes and compared their predicted expression level as transcription per million (TPM) values that were calculated using the known transcript sequence of *P. reticulata* as reference (Dataset S1). RNA-Seq suggested that *cubilin* (*cubn*) and *amnionless (amn*) were highly expressed in the trophotaeniae; however, other co-receptor genes (*lrp1aa*, *lrp2a*) were considerably lower (Figure 1C, Table S1). Adaptor protein-2 (AP2) subunit genes (*ap2a1*, *ap2b1*, *ap2m1a*, and *ap2s1*) were more highly expressed than the other family adaptor genes (*ldlrap1b* and *numb*) (Figure 1C, Table S2). Two families of the vesicle coating protein genes (*clta*, *cltbb*, *cltc*; *flot1b*, *flot2a*) were expressed higher than the vesicle proteins classified in other families (*cav2* and *cav3*) (Figure 1C, Table S3). The lysosomal endopeptidase enzyme gene (*ctsl.1*) exhibited a high TPM value (> 10,000) rather than that of not only protease family genes but also most of the genes expressed in the trophotaeniae (Figure 1C, Table S4). The trend of the predicted TPM values in each gene was not noticeably different between the 3$^{rd}$- and 4$^{th}$- week samples.

*Sequences for Cubam receptor genes*

A Cubam receptor is known to be a membrane-bound multi-ligand receptor consisting of Cubn and Amn (Figure 2A). The secreted protein Cubn specifically binds to the transmembrane protein Amn; thus, the CUB domain that associates with the ligands are localized on the apical surface of the plasma membrane. We obtained the amino acid sequences of *X. eiseni* Cubn and Amn by *de novo* assembly of NGS reads from the trophotaeniae. The sequences for Cubn and Amn were compared between four vertebrate species, *Homo sapiens*, *Danio rerio*, *P. reticulata*, and *X. eiseni.* The binding motifs were conserved in the species (Figure 2B and C). The intracellular domain of Amn included two conserved motifs to bind the adaptor proteins, including AP2. The motifs were also conserved in the species (Figure 2D).

*Distribution of Cubilin and Amnionnless in trophotaenia*

To validate the expression of *cubn* and *amn* in the trophotaenia, semi-quantitative RT-PCR analyses were performed using total RNAs extracted from the whole-embryo including the trophotaeniae, isolated trophotaeniae, and adult skeletal muscle. The muscle sample was used as a control for tissue with low endocytosis activity. The gene expression patterns did not conflict between the results of RT-PCR and RNA-Seq. In the embryo and trophotaenia, both *cubn* and *amn* were more highly expressed than *lrp2a* (Figure 3A). Conversely, no or few expressions of the target genes except *actb* as a positive control were detected in the adult muscle. Next, to detect protein localization, immunohistochemistry was performed using antibodies against Cubn or Amn. In both proteins, strong signals were observed in the epithelial monolayer of the trophotaenia, while few background noises were detected in the control assay (Figure 3B-D, see also Figure S1 and S2). Confocal microscopy revealed the cellular distribution of the anti-Cubn signals. The signals in the apical surface of the epithelial cell were detected as a homogeneous

126 distribution, while almost all signals in the cytoplasm were captured as a dot pattern (Figure 3E, Figure
127 S3). Immunoelectron microscopy revealed that the microvilli were distributed on the apical surface of the
128 trophotaenia epithelium, and intracellular vesicles were observed in the cytoplasm; furthermore, anti-Cubn
129 signals were distributed in the intracellular vesicles and overlapped with the microvilli on the apical surface
130 (Figure 3F).

131

132 *Proteolysis activity in trophotaenia*

133 Cathepsin L is a lysosomal cysteine proteinase characterized by three conserved protease regions and
134 active sites consisting of cysteine, histidine, or asparagine (Figure 4A). The functional regions were
135 conserved in the *X. eiseni* Cathepsin L protein translated from the coding sequence of *ctsl.1*. RT-PCR
136 analysis revealed a strong expression of *ctsl.1* in the trophotaenia (Figure 4B). To identify which type of
137 cells include proteolysis activity in the trophotaenia, acidic organelles including lysosomes and
138 endosomes were detected using a fluorescent probe. The LysoTracker® indicated the presence of acidic
139 organelles in the epithelial layer cells (Figure 4C). The signals were distributed in the cytoplasm and were
140 not components in the nuclei (Figure 4D). According to the RNA-Seq analysis, *ctsl.1* was presumed to be
141 the highest expressed *cathepsin* gene in the trophotaenia; thus, we calibrated the proteolysis activity of
142 cathepsin L in the trophotaenia using a fluorescent substrate-based measurement system. The
143 fluorescence indicating substrate digestion was significantly higher in the trophotaenia lysate than in the
144 control at one h after the reagent mixture. Furthermore, the intensity of the lysate condition continued to
145 increase for 7 h (Figure 4E, Table S5). Conversely, the increase in intensity was strongly suppressed by a
146 cathepsin L inhibitor.

147

148 *Adaptors and vesicle coating proteins*

149 The expression of candidate genes for adaptors (*ap2a1*, *ap2b1*, *ap2m1a*, *ap2s1*, *ldlrap1b*, and *numb*)
150 and vesicle coating proteins (*clta* and *cltc*) were confirmed by RT-PCR (Figure S4). We determined an
151 incomplete transcript for *X. eiseni* Dab2 from the *de novo* assembly; however, it lacked internal sequences
152 in comparison with the proteins in other vertebrates (Figure S5). Furthermore, no amplicons were
153 obtained by RT-PCR using primers designed based on the Dab2-like sequence.

154

## Discussion

RNA-Seq analyses revealed high expression of the genes for receptor-mediated endocytosis in the trophotaenia of *X. eiseni* embryos. Cubn and Amn form a Cubam receptor complex that associates with Vitamin-B12, albumin, transferrin, and other ligands [20,21]. The predicted amino acid sequences for *X. eiseni* Cubn and Amn obtained from the *de novo* assembly both possessed a conserved motif which allowed binding to each other, and Amn retained adaptor binding sites in the intracellular region [21, 22]. Immunohistochemical analysis indicated the presence of Cubn not only in the apical surface of the epithelial layer but also in the intracellular vesicles in the cells, suggesting the incorporation and recycling of endocytic receptors [23,24]. This evidence supports the idea that Cubam plays a role as a receptor for the intraovarian nutrients and is involved in endocytosis. We also indicated the low presence of Lrp2 (also known Megalin), which is a major co-receptor for Cubam [25]. This indicated that Cubam works independently or in cooperation with other co-receptors, except Lrp2, in the trophotaenia. In zebrafish, a previous study reported that Cubam-dependent endocytosis in the lysosome rich enterocytes (LREs) does not require the presence of Lrp2 [19]. This supports our hypothesis; however, we do not exclude the possibility that our sequencing and alignment processes could not catch other *lrp2* orthologous genes in *X. eiseni*. Park et al. [19] also reported that Dab2 is an essential adaptor molecule not only in the zebrafish larval intestine but also in the endocytic nutrient absorption in the ileum of suckling mice. However, we obtained only an incomplete sequence for the *X. eiseni* Dab2-like protein without an internal region compared with mammalian orthologs. This may be an alternative splice form with less endocytic activity [26,27]. Furthermore, we did not detect Dab2-like expression by RT-PCR, and we could not exclude the possibility that the predicted Dab2-like sequence is caused by an assembly error. Thus, the contribution of Dab2 to endocytosis in the trophotaenia has not been confirmed in this study. The other adaptor or vesicle coating proteins we detected were typical co-factors for receptor-mediated endocytosis. Conversely,

178 Caveolin is a vesicle coating protein involved in receptor-independent endocytosis [28]. Thus, a low
179 expression of *caveolin* genes (*cav2* and *cav3*) does not conflict with the activation of Cubam-mediated
180 endocytosis. Additionally, biochemical assays supported that cathepsin L is an active protease that
181 functions in the intracellular vesicles that is configured following membrane budding. This evidence
182 supports the idea that Cubam-mediated endocytosis and cathepsin L-dependent proteolysis is one of the
183 key mechanisms for the absorption of the maternal component in *X. eiseni* embryos.

184 Cubam is also known to be a scavenger receptor involved in nonspecific protein uptake [20]. In this
185 study, we did not determine the Cubam ligands in the trophotaenia. However, the candidates are limited to
186 intraovarian secreted proteins. In several goodeid species, previous studies indicated that the ovarian
187 fluids include various proteins in a pattern similar to that in the blood serum [13,29]. Therefore, several
188 serum proteins, albumen, transferrin, and others known as Cubam ligands, are potential targets in the
189 case of intraovarian nutrient absorption via the trophotaenia. Another possibility is that vitellogenin is also
190 a potential target because it is secreted into the ovarian fluids and is absorbed into the trophotaenia via
191 intracellular vesicles [15]. Another study suggested that the Cubn-Amn-Lrp2 receptor complex is related to
192 transport of yolk proteins, including vitellogenin, in endodermal epithelial cells during chicken yolk sac
193 growth [30]. These reports support the idea that Cubn and Amn are potent candidate molecules for a
194 receptor complex involved in maternal component uptake in the trophotaenia. However, functional
195 analyses such as gene knockout or transgenic technologies used in conventional model animals, such as
196 laboratory mice or small oviparous fish, have not been applied to goodeid fish. For a direct validation of
197 our hypothesis, these reverse genetic methods should also be developed in the viviparous teleost.

198 As described above, endocytosis-mediated nutrient absorption is not limited to the pseudoplacenta of the
199 viviparous fish; it has also been reported in intestinal tissues (Figure 5). In mammals, macromolecule
200 absorption in the intestine is limited to the suckling period [31]. In the stomachless fish, endocytosis-

mediated absorption is considered to continue in part of the intestine for life, because of low digestive activity in the enteric cavity [18]. We found that Cubn and Amn are also distributed in the intestinal epithelial cells of adult *X. eiseni.* (Figure S7). In most invertebrate species, because the extracellular digestive system is primitive, food particles are absorbed into the intestinal cells by vesicle trafficking and degraded by intracellular digestion [32, 33]. Thus, we hypothesize that endocytic nutrient absorption and intracellular digestion are ancestral traits common not only in vertebrates but also in invertebrates, and their importance has decreased in certain vertebrates with development of the extracellular digestive system in the enteric cavity. The ancestor of the goodeid species may have applied the endocytic process to the reproductive system, and then configured the unique hind-gut derived pseudoplacenta for matrotrophic nutrition during gestation [7,34]. To validate our hypothesis, further exhaustive omics analyses using the goodeid species and comparative research using the subfamily Empetrichthyinae, which is the oviparous species most closely related to the viviparous goodeid fish, are required [6,35].

This study is an investigation of species-specific traits based on the transcriptome of a non-conventional model species. The results revealed potential candidate molecules for nutrient absorption in the pseudoplacenta of the viviparous teleost. As August Krogh wrote, this kind of study would be suitable for investigation using the most appropriate species and is unsuitable for verification using alternative models such as viviparous rodents or oviparous teleosts. We believe that this study is an important and fundamental step in understanding the strategic variation of the reproductive system in vertebrates.

## Methods

### *Animal experiments*

This study was approved by the ethics review board for animal experiments at Nagoya University (Approval number: AGR2020028). We sacrificed live animals in minimal numbers under anesthesia according to the institutional guidelines.

### *Fish breeding*

*X. eiseni* was purchased from Meito Suien Co., Ltd. (Nagoya, Japan). Adult fish were maintained in freshwater at 27 °C under a 14:10-h light: dark photoperiod cycle. Fish were bred in a mass-mating design, and approximately 30 adult fish were maintained for this study. The juveniles were fed live brine shrimp larvae, and the adults were fed Hikari Crest Micro Pellets and ultraviolet-sterilized frozen chironomid larvae (Kyorin Co., Ltd., Himeji, Japan). To accurately track the pregnancy period, the laboratory-born fish were crossed in a pair-mating design, and the mating behavior was recorded.

### *Sample collection*

Fish samples were anesthetized using tricaine on ice before the surgical extraction of tissues or embryos. The obtained samples were stored on ice until subsequent manipulations. In this study, we dissected approximately 10 pregnant females and extracted 15–30 embryos in each operation.

239 *RNA-Seq*

240 Total RNA was extracted from trophotaenae of the 3rd or 4th week of the embryo extracted from the
241 pregnant female using the RNeasy Plus Mini kit (QIAGEN). A total of six samples were obtained from
242 three 3rd week embryos and three 4th week embryos. Next-generation sequencing (NGS) was outsourced
243 to Macrogen Japan Corp. (Kyoto, Japan) using NovaSeq6000 (Illumina, Inc., San Diego, CA, USA).
244 Approximately 60 million 150-bp paired-end reads were obtained in each sample. The NGS data was
245 deposited to the DNA Data Bank of Japan (DDBJ, ID: DRA011209). *De novo* assembly and mapping to
246 the reference sequence were performed by CLC Genomics Workbench .(Filgen, Inc., Nagoya, Japan)
247 The published transcript sequences of*Poecilia reticulata* (NCBI Genome, ID: 23338) was used as a
248 reference. The transcript sequences of *X. eiseni* were deposited into the DDBJ. The accession numbers
249 were listed in Table S6.

250

251 *Reverse transcription (RT) PCR*

252 Total RNA was extracted from tissues or whole embryos using the RNeasy Plus Mini kit and reverse-
253 transcribed using SuperScript IV reverse transcriptase (Thermo Fisher Scientific). PCR was carried out
254 using KOD-FX-Neo (Toyobo, Osaka, Japan) under the following conditions: 100 s at 94 °C, followed by 32
255 cycles of 20 s at 94 °C, 20 s at 60 °C, 60 s at 72 °C, and 120 s at 72 °C. Primer sequences are listed in
256 the Resource List in Table S6.

257

258 *Antibodies and antiserums*

Antiserums against Cubn and Amn were generated in this study. The antigen sequences were 6× His-tagged peptide of 151 amino acids (aas) corresponding to the intermediate region of *X. eiseni* Cubn (Accession#, LC595284; aa 691–841) and 6× His-tagged peptide of 247 aas corresponding to the C-terminal of *X. eiseni* Amn (Accession#, LC595285). The experimental procedure has been described in our previous study [15]. All antibodies and antiserums used in this study are listed in Table S7.

*Immunohistochemistry*

Tissue samples were fixed in 4.0% paraformaldehyde/phosphate-buffered saline (PFA/PBS) at 4 °C overnight. Samples were permeabilized using 0.5% TritonX-100/PBS at room temperature for 30 min. Endogenous peroxidase was inactivated by 3.0 % hydrogen peroxide/PBS for 10 min. Then, the sample was treated with Blocking-One solution (Nacalai Tesque, Kyoto, Japan) at room temperature for 1 h. Primary antibody or antiserums were used at 1:500 dilution with Blocking-One solution. Samples were incubated with primary antibody or antiserum at 4 °C overnight. Secondary antibodies were used at a 1:500 dilution in 0.1% Tween-20/PBS. Samples were treated with the secondary antibody solution at 4 °C for 2 h. We performed a 3,3'-Diaminobenzidine Tetrahydrochloride (DAB) color development using the DAB Peroxidase Substrate Kit, ImmPACT (Vector Laboratories, Inc., Burlingame, CA, USA). Microscopic observation was performed using an Olympus BX53 microscope and photographed using a DP25 digital camera (Olympus, Shinjuku, Japan).

*Fluorescent Immunohistochemistry*

Tissue samples were fixed in 4.0% PFA/PBS at 4 °C overnight. Samples were permeabilized using 0.5%

TritonX-100/PBS at room temperature for 30 min. Endogenous peroxidase was inactivated by 3.0 % hydrogen peroxide/PBS for 10 min. Then, the sample was treated with Blocking-One solution (Nacalai Tesque, Kyoto, Japan) at room temperature for 1 h. Primary antibody (anti-Cubn) was used at a 1:500 dilution with Blocking-One solution. Samples were incubated with primary antibody at 4 °C overnight. Secondary antibody was used at a 1:500 dilution in 0.1% Tween-20/PBS with 4',6-diamidino-2-phenylindole (DAPI). Samples were treated with the secondary antibody solution at 4 °C overnight. Microscopic observation was performed using a Leica TCS SP8 microscope (Leica Microsystems, Wetzlar, Germany).

*Immunoelectron microscopy*

Embryo samples were fixed in 4.0% PFA/PBS. Fixed samples were washed in PBS, then reacted with a primary antibody (anti-Cubn) at 4 °C overnight, and then reacted with biotinylated anti-rabbit IgG (Vector, Burlingame, CA, USA) at room temperature for 2 h. Samples were performed with the avidin–biotin–peroxidase complex kit (Vector), and visualized with 0.05% DAB (Dojindo Laboratories, Kumamoto, Japan) and 0.01% hydrogen peroxide in 50 mM Tris buffer (pH 7.2) at room temperature for 10 min. The procedure for electron microscopy is described in our previous study [15].

*Labeling acidic organelles*

The live embryos immediately after extraction from the pregnant female at the 4$^{th}$-week post-mating were incubated in PBS with a 1:1000 dilution of LysoTracker® Red (Thermo Fisher Scientific) for 1 h at room temperature. The samples were fixed with 4.0 % PFA/PBS and stained with DAPI. Microscopic

observation was performed using a Leica DM5000 B microscope (Leica Microsystems, Wetzlar, Germany).

*Measurement of Cathepsin L activity*

The trophotaenia lysate was prepared from six littermate embryos obtained from the pregnant females at the 4$^{th}$-week post-mating. The trophotaeniae were manually extracted from the embryo under a microscope. Proteolysis detection was performed using the Cathepsin L Activity Fluorometric Assay Kit (BioVision, Inc., Milpitas, CA, USA). The fluorescence intensities were measured using a Qubit 4 Fluorometer (Thermo Fisher Scientific).

## Acknowledgments

This work was supported by research grants from the Nakatsuji Foresight Foundation and the Daiko Foundation.

## Data accessibility

The data that support the findings have been provided with the manuscript.

## References


1. A. Krogh, The progress of physiology. *Am. J. Physiol*. **90**, 243-251 (1929).

2. D. Blackburn, “Viviparity and oviparity: Evolution and reproductive strategies” in: Encyclopedia of Reproduction, Vol. 4, E. Knobil, J. D. Neill, Eds. (Academic Press, 1999), pp. 994-1003.

3. G. J. Burton, A. L. Fowden, Review: The placenta and developmental programming: balancing fetal nutrient demands with maternal resource allocation. *Placenta*. **33**, S23-S27 (2012).

4. R. W. Gill, G. Kossoff, P. S. Warren, W. J. Garrett, Umbilical venous flow in normal and complicated pregnancy. *Ultrasound Med. Biol*. **10**, 349-363 (1984).

5. R. M. Roberts, J. A. Green, L. C. Schulz, The evolution of the placenta. Reproduction (Cambridge, England), **152**, R179–R189 (2016).

6. K. L. Foster, K. R. Piller, Disentangling the drivers of diversification in an imperiled group of freshwater fishes (Cyprinodontiformes: Goodeidae). *BMC Evol. Biol.* **18**, 116 (2018).

7. C. L. Turner, Pericardial sac, trophotaeniae, and alimentary tract in embryos of goodeid fishes. *J. Morphol.* **67**, 271-289 (1940).

8. S. M. Tinguely, A. Lange, C. R. Tyler, Ontogeny and Dynamics of the Gonadal Development, Embryogenesis, and Gestation in *Xenotoca eiseni* (Cyprinodontiformes, Goodeidae). *Sex Dev*. **13**, 297-310 (2019).

9. C. L. Turner, Viviparity Superimposed upon Ovo-Viviparity in the Goodeidae, a Family of Cyprinodont Teleost Fishes of the Mexican Plateau. *J. Morphol.* **55**, 207- 251 (1933).

10. C. L. Turner, The trophotaeniae of the goodeidae, a family of viviparous cyprinodont fishes. *J. Morphol*. **61**, 495- 523 (1937).

11. J. Lombardi, J. P. Wourms, The trophotaenial placenta of a viviparous goodeid fish. I. Ultrastructure of the internal ovarian epithelium, the maternal component. *J. Morphol*. **184**, 277-292 (1985).

12. F. Hollenberg, J. P. Wourms, Ultrastructure and protein uptake of the embryonic trophotaeniae of four species of goodeid fishes (Teleostei: Atheriniformes). *J. Morphol*. **219**, 105-129 (1994).

13. F. Hollenberg, J. P. Wourms, Embryonic growth and maternal nutrient sources in goodeid fishes (Teleostei: Cyprinodontiformes). *J. Exp. Zool.* **271**, 379–394 (1995).

14. A. Vega-López, E. Ortiz-Ordóñez, E. Uría-Galicia, E. L. Mendoza-Santana, R. Hernández-Cornejo*, et al.,* The role of vitellogenin during gestation of *Girardinichthys viviparus* and *Ameca splendens*; two goodeid fish with matrotrophic viviparity. *Comp. Biochem. Physiol. Part A Mol. Integr. Physiol*. **147**, 731–742 (2007).

15. A. Iida, H. N. Arai, Y. Someya, M. Inokuchi, T. A. Onuma, *et al*., Mother-to-embryo vitellogenin transport in a viviparous teleost *Xenotoca eiseni*. *PNAS*, **116**, 22359-22365 (2019).

16. J. P. Kraehenbuhl, C. Bron, C., B. Sordat, Transfer of humoral secretory and cellular immunity from mother to offspring. *Curr. Top. Pathol*. **66**, 105–157 (1979).

17. P. C. Moxey, J. S. Trier, Development of villus absorptive cells in the human fetal small intestine: a morphological and morphometric study. *Anat. Rec*. **195**, 463–482 (1979).

18. J. H. Rombout, C. H. Lamers, M. H. Helfrich, A. Dekker, J. J. Taverne-Thiele, Uptake and transport of intact macromolecules in the intestinal epithelium of carp (*Cyprinus carpio L.*) and the possible immunological implications. *Cell Tissue Res*. **239**, 519-530 (1985).

19. J. Park, D. S. Levic, K. D. Sumigray, J. Bagwell, O. Eroglu, *et al*., Lysosome-Rich Enterocytes Mediate Protein Absorption in the Vertebrate Gut. *Dev. Cell.* **51**, 7-20 (2019).

20. P. J. Verroust, H. Birn, R. Nielsen, R. Kozyraki, E. I. Christensen, The tandem endocytic receptors megalin and cubilin are important proteins in renal pathology. *Kidney Int*. 62, 745-756 (2002).

21. G. A. Pedersen, S. Chakraborty, A. L. Steinhauser, L. M. Traub, M. Madsen, AMN directs endocytosis of the intrinsic factor-vitamin B(12) receptor cubam by engaging ARH or Dab2. *Traffic*. **11**, 706-720 (2010).

22. C. Larsen, A. Etzerodt, M. Madsen, K. Skjødt, S. K. Moestrup, C. B. F. Andersen, Structural assembly of the megadalton-sized receptor for intestinal vitamin B12 uptake and kidney protein reabsorption. *Nat. Commun.* **9**, 5204 (2018).

23. E. I. Christensen, H. Birn, P. Verroust, S. K. Moestrup, Membrane receptors for endocytosis in the renal proximal tubule. *Int. Rev. Cytol*. **180**, 237-284 (1998).

24. B. D. Grant, J. G. Donaldson, Pathways and mechanisms of endocytic recycling. *Nat. Rev. Mol. Cell Biol*. **10**, 597-608 (2009).

25. E. I. Christensen, H. Birn, Megalin and cubilin: multifunctional endocytic receptors. *Nat. Rev. Mol. Cell Biol.* **4**, 256-266 (2002).

26. M. E. Maurer, J. A. Cooper, Endocytosis of megalin by visceral endoderm cells requires the Dab2 adaptor protein. *J. Cell Sci*. **118**, 5345-55 (2005).

27. C. V. Finkielstein, D. G. Capelluto, Disabled-2: A modular scaffold protein with multifaceted functions in signaling. *Bioessays*. **38**, S45-55 (2016).

28. T. M. Williams, M. P. Lisanti, The caveolin proteins. *Genome Biol*. **5**, 214 (2004).

29. J. F. Schindler, Structure and function of placental exchange surfaces in goodeid fishes (Teleostei: Atheriniformes). *J. Morphol*. **276**, 991-1003 (2015).

30. R. Bauer, J. A. Plieschnig, T. Finkes, B. Riegler, M. Hermann, W. J. Schneider, The developing chicken yolk sac acquires nutrient transport competence by an orchestrated differentiation process of its endodermal epithelial cells. *J. Biol. Chem.* **288**, 1088-1098 (2013).

31. V. Muncan, J. Heijmans, S. D. Krasinski, N. V. Büller, M. E. Wildenberg, *et al*., Blimp1 regulates the transition of neonatal to adult intestinal epithelium. *Nat. Commun*. **2**, 452 (2011).

32. P. V. Fankboner, Digestive System of Invertebrates. In book: eLS (2001).

33. V. Hartenstein, P. Martinez, Phagocytosis in cellular defense and nutrition: a food-centered approach to the evolution of macrophages. *Cell Tissue Res*. **377**, 527–547 (2019).

34. M. C. Uribe, H. J. Grier, S. A. Avila-Zúñiga, A. García-Alarcón, Change of lecithotrophic to matrotrophic nutrition during gestation in the viviparous teleost *Xenotoca eiseni* (Goodeidae). *J. Morphol*. **279**, 1336-1345 (2018).

35. R. Van Der Laan, W. N. Eschmeyer, R. Fricke, Family-group names of Recent fishes. *Zootaxa*. **3882**, 1-230 (2014).

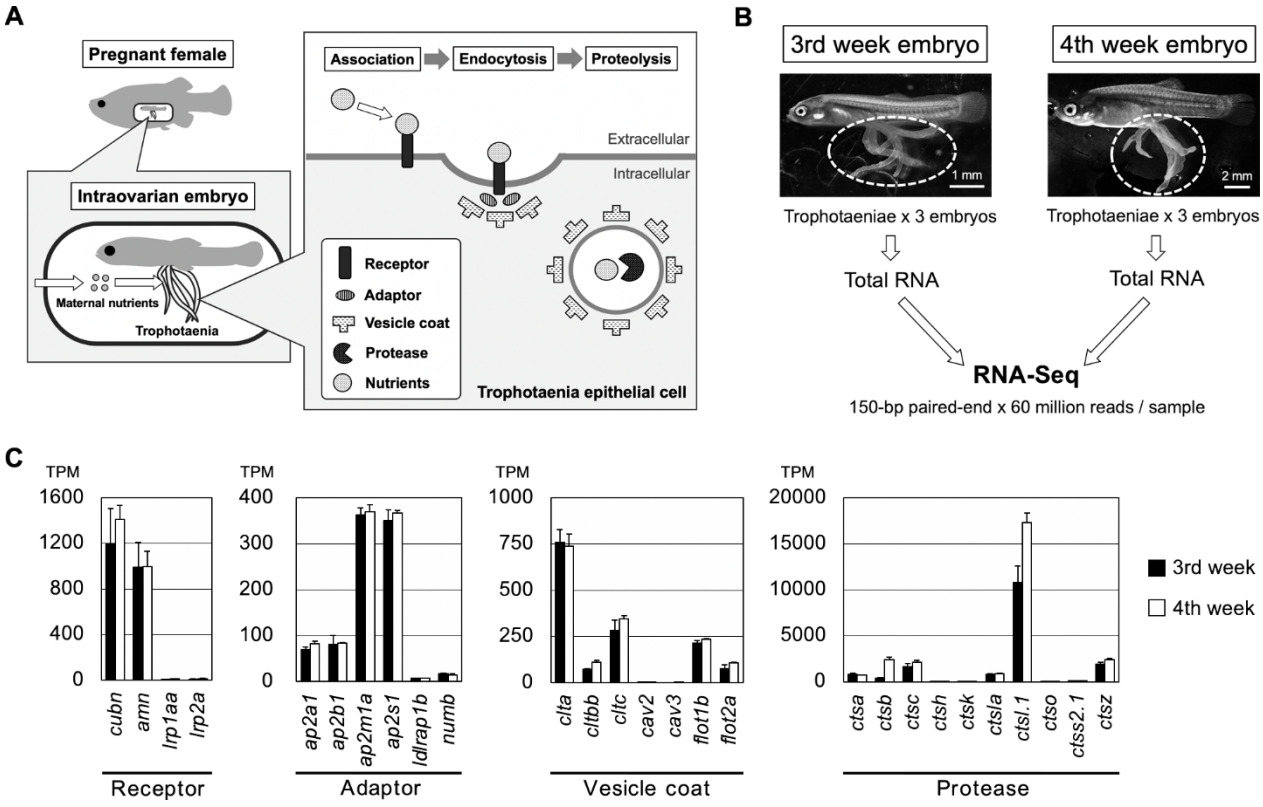


**Figure 1. Exploring candidate genes for nutrient absorption**

**A**. A working model and hypothesis of this study. In the goodeid viviparous fish (*X. eiseni*), intraovarian embryo absorbs maternal nutrients via the trophotaenia. We hypothesized that endocytosis-mediated proteolysis is related to nutrient absorption. Based on the scenario, potential target genes are for endocytic receptors, adaptors, vesicle coating proteins, and proteases. **B**. An experimental scheme for the RNA-Seq analysis. RNA samples were obtained from the trophotaeniae (white dotted line) of the single intraovarian embryos extracted from the pregnant females of the 3rd- or 4th-week post-mating. The RNA-Seq was performed using three samples at every stage. **C**. The graphs indicate the TPM values of the genes selected from the RNA-Seq data that are involved in the endocytosis-mediated proteolysis pathway.

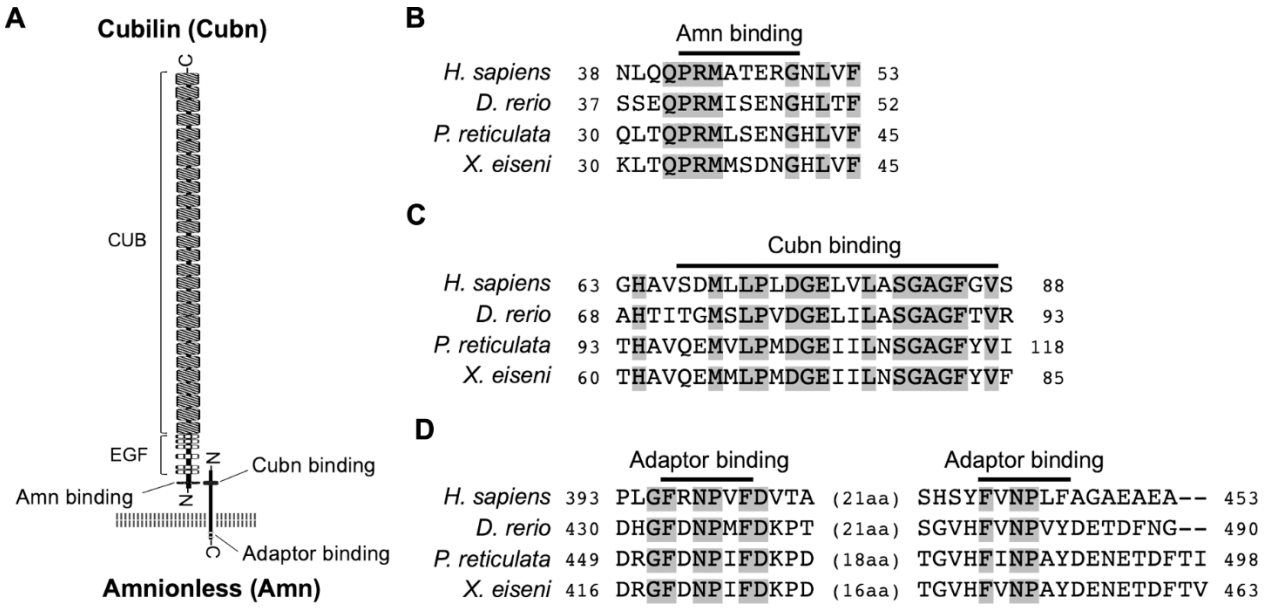


**Figure 2. Structures and amino acid sequences for *X. eiseni* Cubn and Amn**

**A**. The illustration indicates that a typical structure of Cubam receptor complex consists of Cubn and Amn. Both proteins possess a conserved motif to bind each other in the N-terminal regions, and the Amn possesses two adaptor binding motifs in the C-terminal intracellular domain. **B-D**. A comparison of amino acid sequence around the Amn-binding motif in Cubn (**B**), Cubn-binding motif in Amn (**C**), and adaptor binding motifs in Amn (**D**) between *X. eiseni* and three other vertebrate species. The gray filled texts are conserved sequences among the four species.

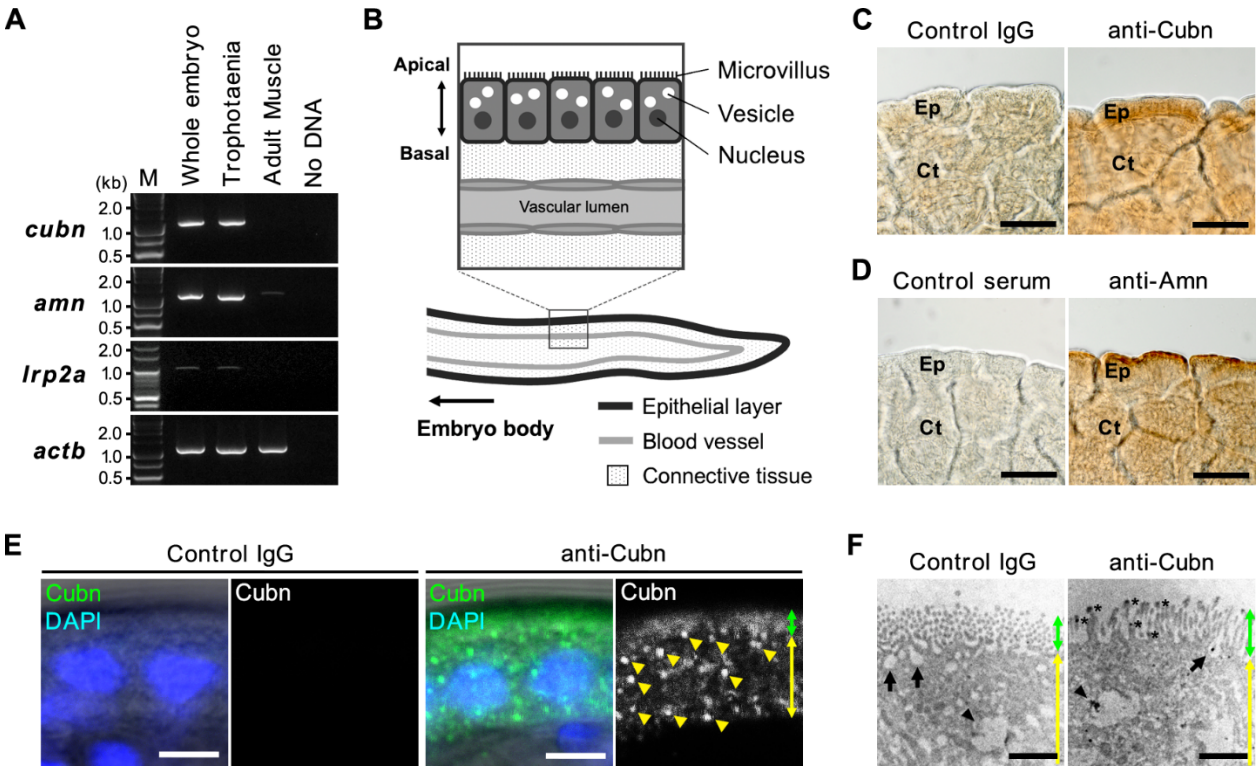


**Figure 3. Distribution of receptors involved in endocytosis**

**A**. RT-PCR for the candidate genes for the receptors involved in the endocytosis. All amplicons were detected as single band on the expected sizes based on the transcript sequences obtained from the *de novo* assembly. **B**. The illustration indicates an internal structure of the trophotaenia. An epithelium cell layer configures an outermost structure of the trophotaenia, which contacts the ovarian luminal fluids. The layer consists of an enterocyte-like cell with microvilli on the apical surface and vesicles in the cytoplasm. **C-D**. Immunohistochemistry using the Cubn antibody or Amn antiserum in the trophotaenia. In both samples, DAB color development was observed in the epithelial layer. Ep, epithelial layer. Ct, connective tissue. Scale bar, 50 μm. **E**. Confocal microscopy images of fluorescent immunohistochemistry using the Cubn antibody in the epithelial layer cells. Yellow triangles indicate the dotted signals in the epithelial cells of the trophotaenia. Green double-headed arrow indicates the apical surface defined by the flat signal.

Yellow double-headed arrow indicates the cytoplasmic region including the dotted signals. Scale bar, 5 μm. **F.** Immunoelectron microscopy using the Cubn antibody in the epithelial layer cells. Green double-headed arrow indicates the microvilli on the apical surface. Yellow double-headed arrow indicates the cytoplasmic region including the dotted signals. Asterisks indicate anti-Cubn signals in the microvilli. Arrows indicate endocytic vesicles in the invagination phase. Arrowheads indicate intracellular vesicles after endocytosis. Anti-Cubilin signals were observed in both vesicles. Scale bar, 1 μm.

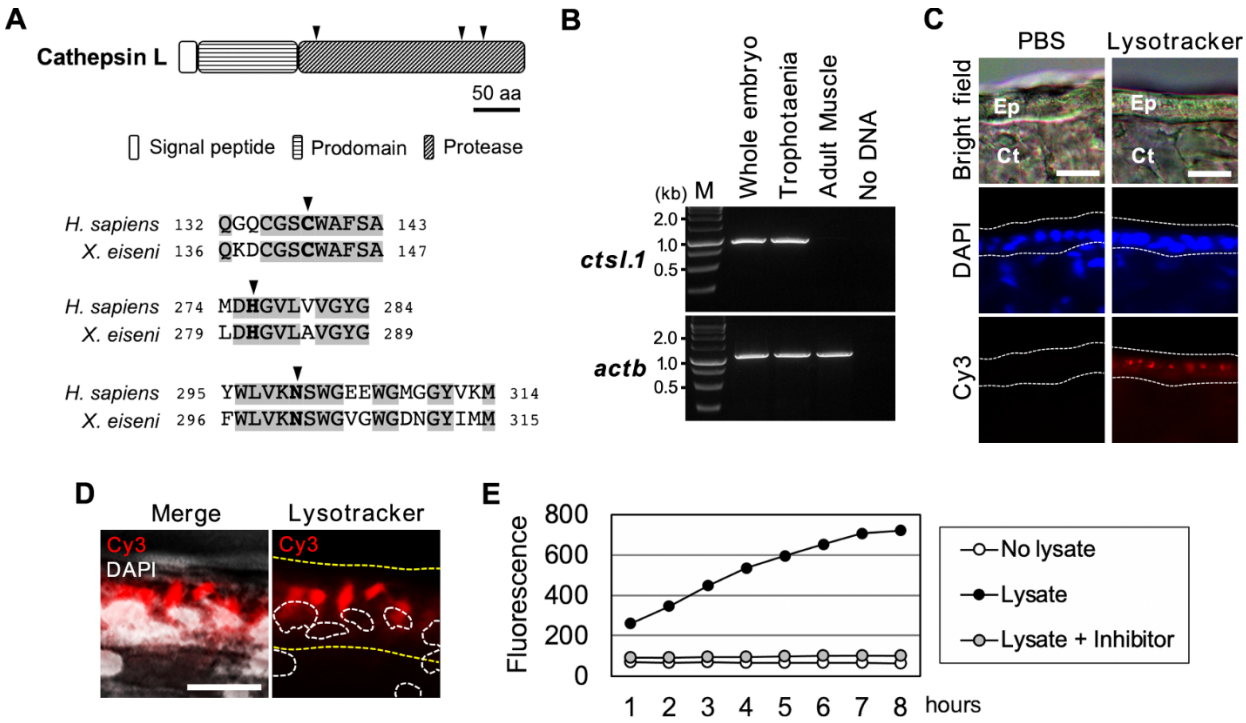


**Figure 4. Proteolysis activities in trophotaenia**

**A**. The illustrations indicate a typical structure of cathepsin L and a comparison of the protease domains of cathepsin L between *H. sapiens* and *X. eiseni*. The gray filled texts are conserved sequences among the species. The black triangles indicate protease active sites. **B**. RT-PCR for *cstl.1* exhibited the highest TPM value in the RNA-Seq analysis. The amplicons were detected as a single band on the expected size based on the transcript sequences obtained from the *de novo* assembly. **C**. Labeling of acidic organelles including lysosomal vesicle in the trophotaenia. The lysotracker treatment exhibited red fluorescence in the epithelial layer (white dotted line). Ep, epithelial layer. Ct, connective tissue. Scale bar, 20 μm. **D**. High magnification image of the lysotracker-treated epithelial cell layer of the trophotaenia. Yellow dotted line indicates the epithelial layer and white dotted circles are the nuclei of the epithelial cells. The lysotracker fluorescence was observed in the cytoplasm. Scale bar, 10 μm. **E**. Measurement of cathepsin L activity based on fluorescent substrate degradation. The vertical line indicates the accumulation of cleaved fluorescent substrates, which means cathepsin L activity in the sample solution. The fluorescent value of

488 the trophotaenia lysate sample was increased by 8 h after the reaction started.

489

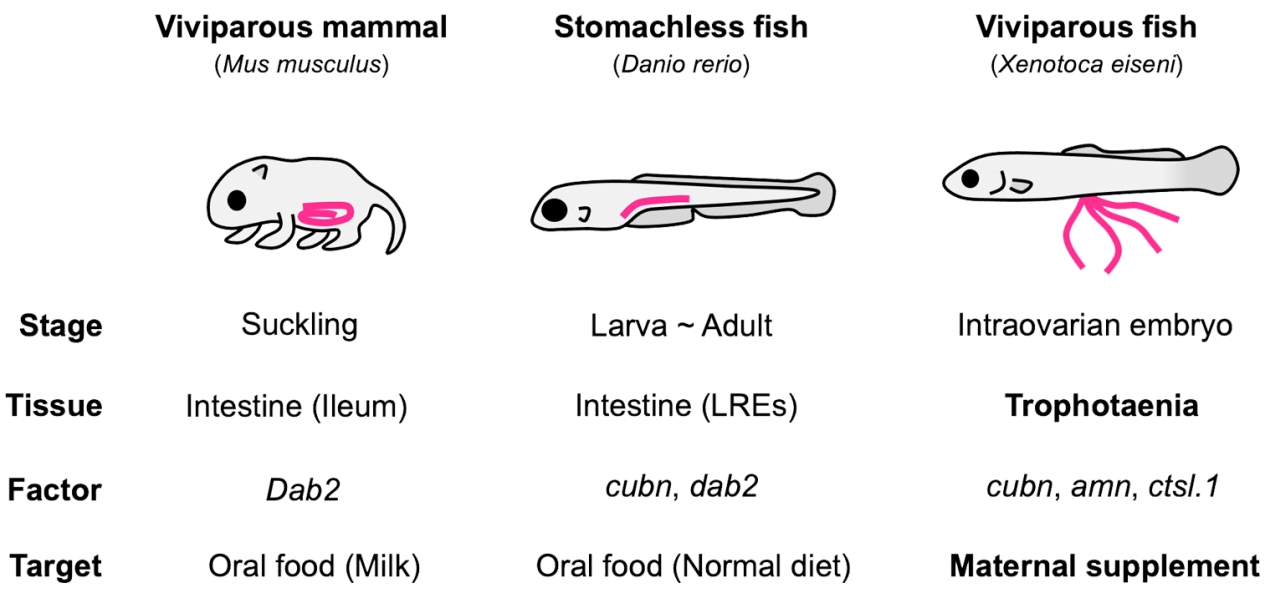


**Figure 5. Comparison of endocytosis-mediated nutrient intake in vertebrates**

Endocytosis-mediated nutrient intake has also been reported in a viviparous mammal and stomachless fish. In these species, oral ingestion macromolecules are absorbed from a region of the intestine via endocytosis. In contrast, intraovarian embryos of the viviparous fish (family Goodeidae) absorbs the maternal component in the ovarian fluids from the trophotaeniae via endocytosis. Endocytosis in each species is predicted to be driven by similar molecular process in the enterocytes of the intestine or the enterocyte-like cells of trophotaenia; however, the biological ontology would be divergent between the viviparous fish (intraovarian growth) and the others (feeding after birth).